

A three-dimensional elastoplastic analysis of mixed-mode K_I/K_{II} around the crack front

*Luiz Fernando Nazaré Marques*¹, *Jaime Tupiassú Pinho de Castro*², *Luiz Fernando Martha*², and *Marco Antonio Meggiolaro*²

¹Federal University of South and Southeast of Pará, UNIFESSPA, Avenida dos Ipês s/n, Marabá, 68500-000, Brazil

²Pontifical Catholic University of Rio de Janeiro, PUC-Rio, Rua Marquês de São Vicente 225, Rio de Janeiro, 22451-900, Brazil

Abstract. Engineering problems that involve fatigue crack growth and fracture frequently can be studied by taking into account only mode-I features. However, many important problems that involve combined mode I and II loadings cannot be properly analyzed by a pure mode-I approach, which in particular may not be sufficient to estimate fracture toughness for practical purposes in such cases. Such mixed-mode problems involve crack orientation and/or load conditions that lead to combined local Stress Intensity Factors (SIFs) K_I/K_{II} around the crack front. Using multiaxial crack tip condition characterized by the crack inclination angle β in a mixed-mode K_I/K_{II} modified single edge tension SE(T) specimen, such mixed-mode effects on plastic zone shapes, volumes and plastic work U_{PL} are taken into account to evaluate problems that involve fatigue and fracture.

1 Introduction

Elastoplastic (EP) stress/strain fields around crack tips are most important in structural integrity evaluations. Damage accumulated on them is the actual driving force for failure mechanisms such as fatigue crack growth (FCG), stable crack tearing, unstable fracture, and even environment assisted cracking. Since cracks prefer to grow perpendicularly to the main principal stress (at least when it is tensile), probably most engineering problems that involve FCG can be properly modelled by taking into account only mode-I features. However, there are many important problems where the combined effect of mixed mode I and II loadings cannot be neglected. In particular, a pure mode-I approach may not be sufficient to estimate fracture toughness for practical purposes in such cases. Such mixed-mode problems involve crack orientation and/or load conditions that lead to non-negligible combined local Stress Intensity Factors (SIFs) K_I/K_{II} around the crack front. Therefore, it is almost a

¹Corresponding author: lfernando@unifesspa.edu.br

truism to claim that analyses of cracked components that induce mixed-mode conditions around the crack tip under multiaxial stress states are needed to properly evaluate their fatigue and fracture behavior.

It is well known that geometric parameters, loading conditions, and transversal constraints can affect plastic zone (pz) sizes and shapes. Indeed, for instance under pure mode I conditions, a same SIF value K_I can provide different pz sizes and shapes in thin or thick components due to plane stress or plane strain conditions along the crack front. This effect occurs because of transversal displacement constraints around the crack tip in thick components, which may restrict the pz formation by inducing higher localized hydrostatic stress components (in comparison to the plane stress conditions prevalent in thin cracked components). In the case of pure mode I loadings, there is a number of detailed 3D numerical studies to quantify pz effects on the structural integrity of cracked mechanical components, see e.g. [1-4].

However, what certainly is less well-known is that pz sizes and shapes can be much affected as well by equally important effects of nominal load to yield strength σ_n/S_Y and of crack size to component width a/W ratios. Such effects are simply neglected in traditional pz estimates, which assume pzs depend only on the driving force (the SIF K under linear elastic (LE) or the equivalent J -integral under elastoplastic (EP) conditions) and on the cracked component thickness, although improved estimates can clearly identify at least the σ_n/S_Y effects [5]. Therefore, it should not be a surprise that traditional pz estimates, as well as structural integrity evaluations based on idealized SIF-dominated stress/strain fields, can be highly inaccurate and thus useless for many practical applications.

Moreover, probably due to the widespread use of traditional pz estimates, σ_n/S_Y and a/W effects are not properly evaluated or even considered in many numerical studies either. To show how inappropriate this practice can be, a recent work [6] used extensive 3D incremental EP numerical simulations to calculate the plastic work U_{PL} dissipated inside the pzs under a same K_I value but different σ_n/S_Y and a/W conditions. That work quantitatively evaluates the use of U_{PL} to estimate the onset of crack tearing in practical EP fracture applications, and presents some experimental evidence that supports such simple and physically appealing idea. In fact, σ_n/S_Y and a/W effects can explain the huge dispersion of EP fracture toughness measurements because, from a physical point of view, the toughness should be controlled by U_{PL} since the work spent to create two new crack faces is much smaller than it in tough materials. The present work extends to mixed mode I-II problems the idea that U_{PL} can and (at least in the authors' opinion) should be used to quantify EP toughness in practical applications, in particular because its numerical calculation by EP finite element procedures, even though not a trivial task, is not a major barrier nowadays.

Experimental photoelastic results and 2D numerical studies under mixed mode I-II configurations are well detailed elsewhere [7-9]. To explore 3D effects on mixed mode I-II problems, the influence of crack tip plastic zones, SIFs, and crack inclination angles β , as well as of σ_n/S_Y and a/W ratios, is numerically investigated by studying a modified single edge tension (SE(T)) specimen [10].

To do so, this work describes and uses an improved methodology for evaluating 3D pz volumes around crack fronts based on 3D EP submodeling finite element (FE) techniques proposed and detailed studied elsewhere [6]. This methodology can be used to eval-

uate cracked components under different transversal constraint levels. These constraints are varied changing the specimen geometry and loading conditions. Geometry parameters are represented by crack length-to-specimen width a/W and specimen width-to-specimen thickness W/B ratios. Loading conditions specified by a given K_I or combined K_I/K_{II} ratios consider they can be induced by different nominal stress-to-yield strength σ_n/S_Y ratios. Multiaxial loading conditions are considered by varying the crack inclination angle β (in radians) in a modified mixed-mode K_I/K_{II} single edge tension SE(T) specimen [9], see Fig. 1.

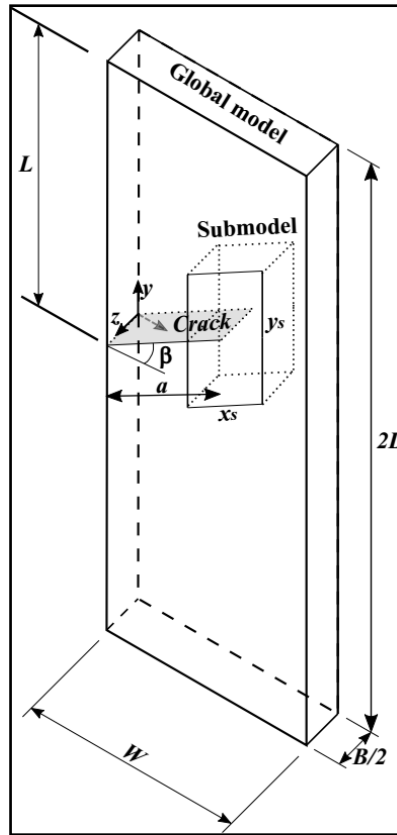


Fig. 1. Some characteristics of the global models and sub-models used to study the mixed mode I–II behavior of a modified single edge tension SE(T) specimen.

2 Finite Element Analysis

A modified SE(T) specimen is considered in this study to simulate mixed mode I–II loading conditions by simply varying the crack angle β , as depicted in Fig. 1. The specimen width is W , its height is $2L$, the thickness is B , and the crack length is a . Pure mode I loading conditions are achieved when $\beta = 0^\circ$. This modified SE(T) specimen is supposed to carry a nominal purely tensile stress σ_n at its upper extremity ($y = L$), assuming a uniformly distributed load P per unit area $W \cdot B$ in the y -axis direction. The lower SE(T) extremity ($y = -L$) is assumed fixed in all degrees of freedom. First, the submodel loading conditions are ob-

tained from the numerical solution of the global model, assuming its material is LE and using proper elements to globally describe its crack.

The submodel dimensions are chosen to assure LE conditions all around its perimeter. All numerical FE calculations are performed considering only 1/2 of the submodel, since it is specified to maintain symmetry about its xy -plane (z -axis). Then, refined incremental 3D EP FE calculations are performed in the submodel to obtain the desired pz shapes as well as the plastic work U_{PL} performed inside them. The Ansys Parametric Design Language (APDL) is used to solve these problems. Further details about the pure mode I numerical problem can be found in [6].

The properties of the materials used in all simulations are presented in Table 1 [10, 11], where E is Young's modulus, ν is Poisson's coefficient, S_Y is yielding strength, while H and h are the monotonic Ramberg-Osgood strain hardening coefficient and exponent.

Table 1. Materials and properties.

Material	E (GPa)	ν (-)	S_Y (MPa)	H (MPa)	h (-)
Elastic isotropic [6]	207	0.3	500	-	-
API 5L X80 [10]	207	0.3	560	892	0.08

2.1 FE Model

The numerical procedure involves two calculation steps. First, the global model with a relatively coarse FE mesh is numerically solved to quantify the LE stress field inside it considering the inclined crack effect. This requires the use of proper elements to simulate the crack tip behavior but, besides that, it poses no major problems. Then, a submodel that contains the crack tip and large enough to contain its desired pz is chosen assuring LE conditions around its perimeter, which are used as its loading conditions. Finally, this submodel is remeshed using a much more refined mesh, to assure the required accuracy can be achieved when numerically incrementally solving its EP stress/strain fields.

The pz 3D EP frontiers are mapped in terms of the equivalent Mises strain ε_{eq} . Quadratic elements (3D SOLID186) are used in these FE simulations, and only the fractions of the volumes corresponding to their plastified Gauss integration points are counted as part of the 3D pz around the crack fronts ($\varepsilon_{eq} \geq \varepsilon_Y$). Hence, the smallest unit of volume considered in the pz models and in the calculation of the plastic work U_{PL} performed inside them became 1/8 of the total volume of the element [6].

When this modified SE(T) specimen with an inclined crack (which provides mixed mode I–II conditions simply by varying its crack inclination angle β) is large and its residual ligament is much larger than its crack size, there are well-known, easy to deduce analytical expressions for its SIFs K_I and K_{II} . When the modified SE(T) residual ligament it is not much larger than a , see e.g. [10], the general expression for its K_i is given by [10]:

$$K_i = \sigma \sqrt{a} f_i g_i \quad (1)$$

where σ is the nominal tensile stress applied in the cracked specimen upper boundary, see Fig. 1, f_i and g_i are geometry factors that depends on the crack size-to-specimen width a/W ratio and on α_i , δ_i and γ_i parameters defined below, with $i = I$ or II , namely:

$$g_I = \cos^2 \beta \quad (2)$$

$$g_{II} = \cos \beta \sin \beta \quad (3)$$

$$f_i \left(\frac{a}{W}, \alpha_i, \delta_i, \gamma_i \right) = \gamma_i \left[\cos \left(\frac{a}{W} \right) \right]^{-\delta_i} + \alpha_i \left(\frac{a}{W} \right) \quad (4)$$

$$\alpha_I = \frac{1.12}{\beta^3 - 0.73\beta^2 + 0.8} \quad (5)$$

$$\delta_I = \frac{8.53 - 5.57\beta}{\beta^2 - 0.82\beta + 1.37} \quad (6)$$

$$\gamma_I = 1.9 \cos \beta^{-0.921} - 0.38\beta^{2.03} \quad (7)$$

$$\alpha_{II} = 0.8\beta^3 - 2.53\beta^2 + 1.66\beta + 0.54 \quad (8)$$

$$\delta_{II} = 2.85\beta^3 - 6.4\beta^2 + 5.1 \quad (9)$$

$$\gamma_{II} = 1.2 \cos \beta^{-0.3} - 0.15\beta \quad (10)$$

The geometric parameters used in this work are $W = 50$ mm, $L = 2W$ and $W/B = 6.25$. Four values for the crack inclination angle β are considered here: 0° (pure mode I), 20° , 40° and 60° . Six a/W ratios are considered as well, namely 0.2, 0.3, 0.4, 0.5, 0.6 and 0.7. Numerical results for both LE and EP materials are presented in Table 2.a and 2.b, considering the properties listed in Table 1. In all these cases, the pz frontiers are evaluated on the surface of specimens. Then, the detailed incremental 3D EP FE calculations are performed in the submodels only for two cases: 1) $a/W = 0.2$, $\beta = 40^\circ$, and $\sigma_r/S_Y = 0.4$; and 2) $a/W = 0.7$, $\beta = 60^\circ$, and $\sigma_r/S_Y = 0.4$.

The 3D LE model is validated for pure mode-I loading conditions (i.e., for cracks with $\beta = 0^\circ$) in [6]. The validation of this new study (for cracks with $\beta > 0^\circ$) is performed considering similar numerical results presented by Wilson [7] and by Merah and Albinmousa [8]. The pz calculated here are compared as well with experimental results presented by Khan et al [10] (only on the surface) and by Albinmousa et al [9].

3 Results

Tables 2.a and 2.b summarize the shapes and sizes of the EP pz frontiers numerically calculated on the surface of the modified SE(T), following all the procedures discussed in the

previous section. They list all crack length-to-width (a/W), nominal load-to-yield strength (σ_n/S_Y), and crack inclination angle β combinations studied here. All the results obtained for pure mode-I ($\beta = 0^\circ$ and $K_{II}/K_I = 0$) are calculated assuming a fixed SIF $K_I = 100 \text{ MPa}\sqrt{\text{m}}$, a value well below the toughness of the API 51 X80 steel, so they can be directly compared without any crack tearing concern.

When the crack angle β increases for each crack size-to-width ratio a/W , the drawings presented in those Tables illustrate how the size and the shape of the pzs vary as K_I reduces and K_{II} increases. The EP pz frontiers are properly scaled to allow the direct comparison between the various cases that have a same a/W .

Table 2.a. Shape and size of the plastic zone on the surface of specimen.

β ($^\circ$)	$a/W = 0.2$			$a/W = 0.3$			$a/W = 0.4$		
	$\sigma_n/S_Y = 0.4, 0.6, 0.82$	$\sigma_n/S_Y = 0.3, 0.55, 0.6$	$\sigma_n/S_Y = 0.3, 0.55, 0.6$	$\sigma_n/S_Y = 0.3, 0.55, 0.6$	$\sigma_n/S_Y = 0.3, 0.55, 0.6$	$\sigma_n/S_Y = 0.3, 0.55, 0.6$	$\sigma_n/S_Y = 0.3, 0.38, 0.6$	$\sigma_n/S_Y = 0.3, 0.38, 0.6$	$\sigma_n/S_Y = 0.3, 0.38, 0.6$
	K_I (MPa)	K_{II} (MPa)	K_{II}/K_I (-)	K_I (MPa)	K_{II} (MPa)	K_{II}/K_I (-)	K_I (MPa)	K_{II} (MPa)	K_{II}/K_I (-)
0	100	0	0	100	0	0	100	0	0
20		19.1	0.19		18.4	0.18		17.4	0.18
40		28.6	0.29		26.6	0.29		24.0	0.28
60		25.6	0.39		22.5	0.39		19.1	0.39

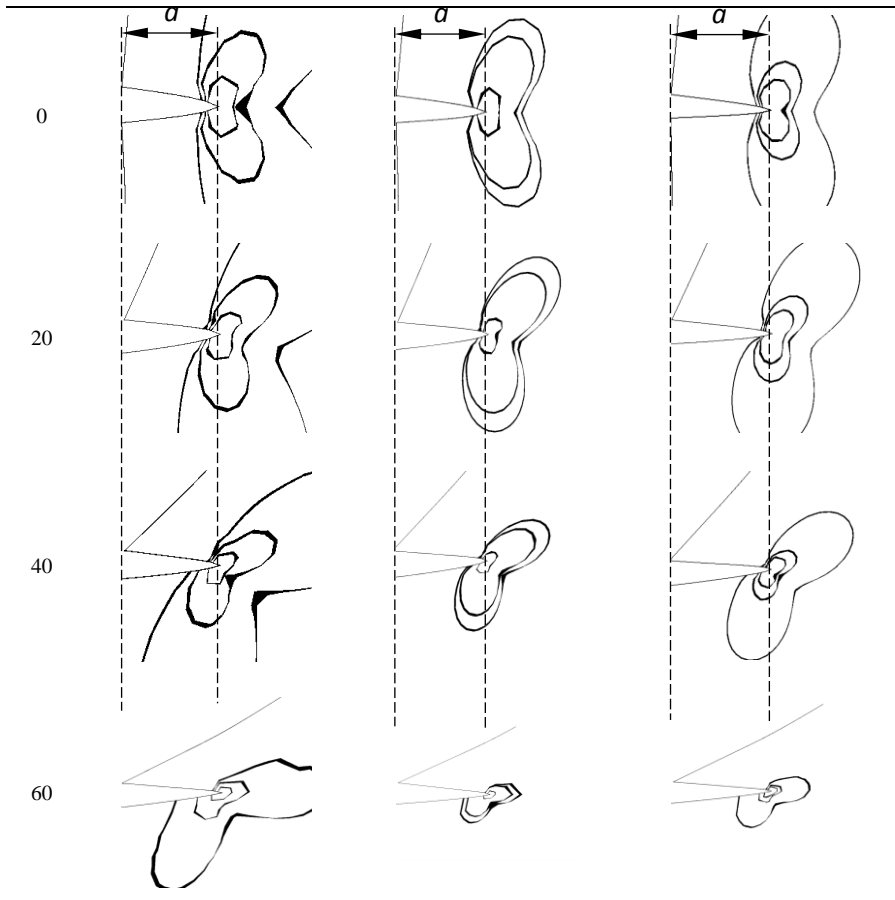
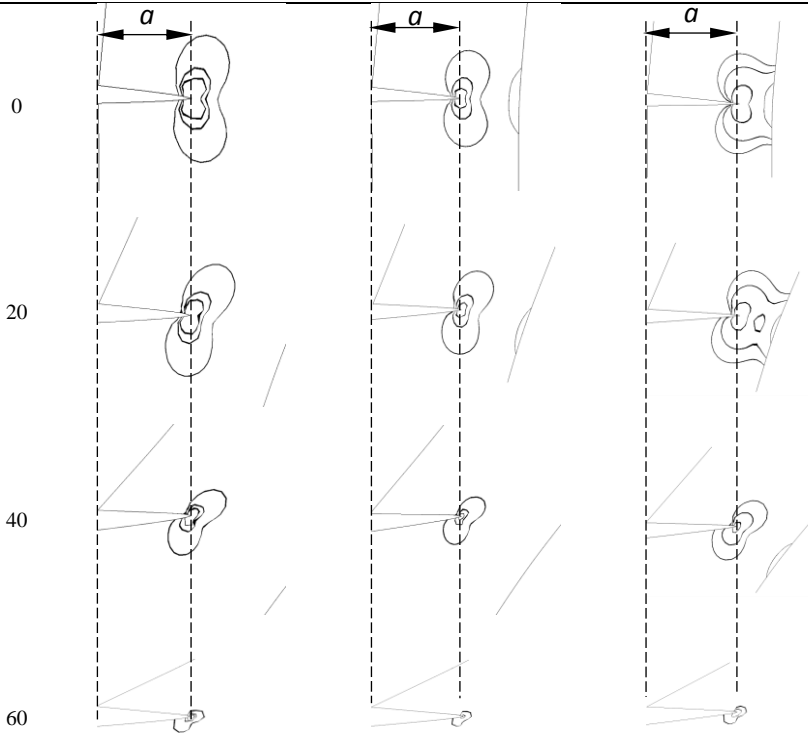


Table 2.b. Shape and size of plastic zone on the surface of specimen.

β (°)	$a/W = 0.5$			$a/W = 0.6$			$a/W = 0.7$		
	$\sigma_r/S_Y = 0.2, 0.25, 0.4$			$\sigma_r/S_Y = 0.1, 0.16, 0.3$			$\sigma_r/S_Y = 0.1, 0.2, 0.3$		
	K_I (MPa)	K_{II} (MPa)	K_{II}/K_I (-)	K_I (MPa)	K_{II} (MPa)	K_{II}/K_I (-)	K_I (MPa)	K_{II} (MPa)	K_{II}/K_I (-)
0	100	0	0	100	0	0	100	0	0
20		16.2	0.17		14.7	0.16		12.9	0.15
40		21.0	0.27		17.6	0.26		14.0	0.25
60		15.5	0.38		11.9	0.37		8.6	0.37



The results based on 3D pz volumes around crack fronts are presented here in order to be explored as a new approach to estimate the resistance to crack tearing initiation. The pz volumes of the two cases using the 3D EP FE calculations are presented in Fig. 2. The volumes V_1 , V_2 and the ratio between them V_2/V_1 are 123 mm³, 766 mm³ and 6.23, respectively.

As the fracture resistance depends on geometric parameters, loading conditions, and transversal constraints, which much affect pz sizes and shapes, and thus the U_{PL} spent inside the pz . Hence, from a physical point of view, it is at least reasonable to assume that the toughness of most metallic cracked structural components depends primarily on the U_{PL}

spent inside the pz . For the same cases, the plastic work $U_{PL,1}$, $U_{PL,2}$ and the ratio between them $U_{PL,2}/U_{PL,1}$ are 92 mJ, 936 mJ and 10.2, respectively. However, to validate these numerical estimations, comparisons between the U_{PL} spent inside the pz volume and experimental fracture toughness for mixed-mode K_I/K_{II} conditions should be made.

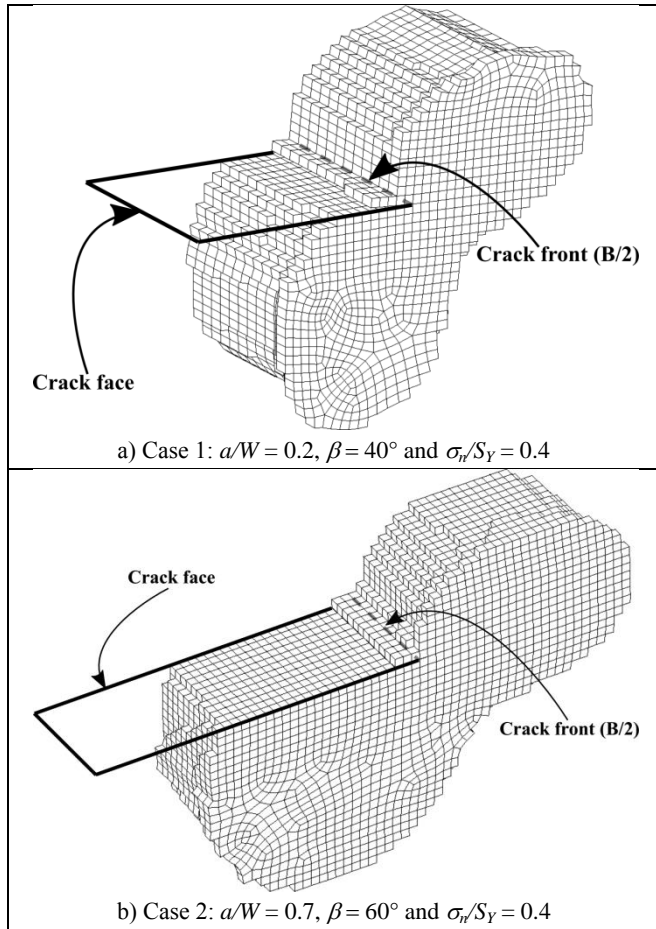


Fig. 2. 3D plastic zone volumes: a) V_1 , and b) V_2 .

4 Conclusions

In this work three-dimensional elastic and elastoplastic finite element analyses have been used to generate numerical predictions of plastic zone sizes, shapes, frontiers and volumes in a modified SE(T) specimen with an inclined crack for both standard pure mode I ($\beta = 0^\circ$) and for mixed mode I–II ($\beta > 0^\circ$). As the crack inclination angle β increases, the plastic zone size and shape reduces and becomes non-symmetrical about the crack length/front, respectively. Plastic zone size increases with increasing crack length of the specimen and nominal stress-to-yield strength σ_n/S_Y ratios. For relative high σ_n/S_Y ratios combined with large crack lengths, the plastic zone size may increase and become larger and add to the

plastified volume developed near the back of specimen. Hence, all these effects in plastic zone should be taken into account in order to evaluate problems that involve fatigue and fracture. Finally, the approach based in 3D plastic zone volumes and the plastic work dissipated inside them may be a useful tool to replace unreliable combinations based on K and other constraint parameters.

The authors would like to thank the Brazilian funding agency CAPES for the scholarship granted.

References

1. M. Besel, E. Breitbarth. *Advanced analysis of crack tip plastic zone under cyclic loading*. Int J Fatigue, **93**: 92–108 (2016)
2. D. Camas, J. Garcia-Manrique, A. Gonzalez-Herrera. *Numerical study of the thickness transition in bi-dimensional specimen cracks*. Int J Fatigue, **33**: 921–928 (2011)
3. D. Camas et al. *Numerical and experimental study of the plastic zone in cracked specimens*. Eng Fract Mech, **185**: 20–32 (2017)
4. F. Yusof. *Three-dimensional assessments of crack tip constraint*. Theor Appl Fract Mech, <https://doi.org/10.1016/j.tafmec.2019.01.025> (2019)
5. R.A. Souza, J.T.P. Castro, A.A.O. Lopes, L.F. Martha. *On improved crack tip plastic zone estimates based on T -stress and on complete stress fields*. Fatigue Fract Eng Mater Struct, **36**: 25–38 (2013)
6. L.F.N. Marques, E.E. Cota, J.T.P. Castro, L.F. Martha, M.A. Meggiolaro. *On the estimation of the elastoplastic work needed to initiate crack tearing*. Theor Appl Fract Mech, **101**: 80–91 (2019)
7. W.K. Wilson. *On combined mode fracture mechanics*. Research report 69-1E7-FMECH-R1. Westinghouse Research Laboratories, Pittsburgh (1969)
8. N. Merah, J. Albinmoussa. *Experimental and numerical determination of mixed mode extension angle*. ASTM J Test Eval, **37**: 95–107 (2008)
9. J. Albinmoussa et al. *A model for calculating geometry factors for a mixed-mode I–II single edge notched tension specimen*. Eng Fract Mech, **78**: 3300–3307 (2011)
10. S.M.A. Khan, N. Merah, M.J. Adinoyi. *3D effects on crack front core regions, stress intensity factors and crack initiation angles*. Int J Solids Struct, **50**: 1449–1459 (2013)
11. G. Shen, W.R. Tyson, A. Glover, D. Horsley. *Constraint effects on pipeline toughness*. Proc 4th Int Conf Pipeline Tech, **2**: 703–720 (2004).